# Impedance Characterization of Dielectric and semiconducting materials with Organic Capacitors for Organic Transistors

C. M. Li*, L. K. Pan* , C. Q. Sun*, J. Zhang**, and Dan Gamota**
*School of Electrical and Electronic Engineering, Nanyang Technological University, Nanyang Avenue, Singapore 639798
**PRRC, Motorola Labs,, 1301 E. Algonquin Rd., m/d 1014, Schaumburg, IL 60196, USA

## ABSTRACT

A new characterization method based on impedance frequency response analysis at different temperatures has been developed to assess and identify the dielectric and semiconductor materials for organic field-effect transistors (OFET). This method can not only characterize simultaneously dielectric and conductive behaviors of materials but also distinguish individual contributions to electrical conduction or to polarization from layers such as dielectric layer, semiconductor layer, and interfaces in OFET. Two kinds of materials, Urathan and DuPont 5018A as dielectric materials have been used to make a multilayer organic capacitor. It has been observed that Urathan, due to its lower conductivity, non-metallic conduction behavior at high temperature, and lower interfacial resistance, is more suitable as dielectric layer for OFET. Urathan appears an enhancement in conductivity by heating following an Arrhenius law with an activation energy transition from 0.002 to 0.24 eV at ~307 K, which originates from band tail hopping that occurs around the Fermi edge. At ~314 K, a dielectric transition also occurs, which is interpreted as a combination of electron polarization associated to the band tail hopping. The materials were used to fabricate OEFT, which performance was in agreement with that obtained from impedance analysis of the organic capacitor.

***Keywords***: Impedance measurements, dielectric materials, organic transistor, organic capacitor, equivalent circuit

## 1 INTRODUCTION

For more than a decade, Organic field effect transistors (OFETs) have been envisioned as an emerging technology to have great potentials used in applications such as smart cards, flexible display, electronic packaging, memory chips and microsensors, which could have advantages over conventional inorganic transistors in terms of flexible substrate, simple fabrication processes, and especially low manufacturing cost.

Organic material based transistors and their devices often have problems in material degradation and low performance. Investigation of materials is particularly essential. An all organic OFET needs organic dielectric, semiconducting and conducting materials to form dielectric layer, semiconducting gap, gate, source, and drain electrodes. All organic OFETs are very attractive since they can enable low cost printing manufacturing process for low cost electronic components and devices. Extensive research has been conducted to synthesize new high performance organic or polymeric semiconducting and dielectric materials for printing process. Nanometal organic inks are also developed for printed OFET electrodes and conducting transmission lines. Thus, there are lot of new materials These research efforts involve huge works to characterize the developed materials for their performance in OFETs. Conventional approach is to fabricate transistor structures for characterization of the properties of organic materials by I-V or C-V curves [1-3]. The method is tedious and expensive, and cannot distinguish the individual contributions from different layers in the two or multiple layers structure of OFET. In addition, a little attention has been given yet on the effect of temperature on the electronic properties. It is necessary to develop new efficient, simple and inexpensive analysis methods to screening and characterizing different materials for OFETs. It has been known that impedance measurement is an important tool for simultaneous dielectric and conductive characterization of materials. The technique has been widely employed to characterize the dielectric and conductive behavior of ceramic [4], glass [5], nanomaterials [6-8] and organic materials [9-11] in energy storage systems and electronic components through their electrical analogs [12]. In conjunction with structural characterization, impedance analysis yields a complete physical picture of various phenomena occurring in the specimen under different conditions. The most important advantage of impedance measurements is that they can distinguish individual contributions to electrical conduction or to polarization at different interfaces. In this paper, we report a simple way to fabricate multilayer capacitors with organic semiconducting and dielectric materials following by impedance frequency response analysis measurements for characterization and identification of material systems for OFETs.

## 2 EXPERIMENTALS

Urathan and DuPont 5018A were purchased from Aldrich and DuPont, respectively, and used as received.

Since the OFET could basically be considered as a parallel multilayer plate capacitor, where the gate electrode is electrically insulated, via a dielectric layer, from the semiconductor layer, we fabricated an organic capacitor

structure as shown in Figure 1(a), for the assessment and characterization of novel materials for OFET.

The impedance measurements were performed over a frequency range of 1.0 kHz–1.0 MHz from $233^0$ K to $353^0$ K in $10^0$ K steps with an applied potential of 50 mV. Solartron 1260 + 1294 impedance frequency response analyzer was used. The temperature was held for 0.5 h prior to each measurement. All measurements were carried out in atmospheric ambient. Silver paste and/or copper sheet were used as the ohmic contacts.

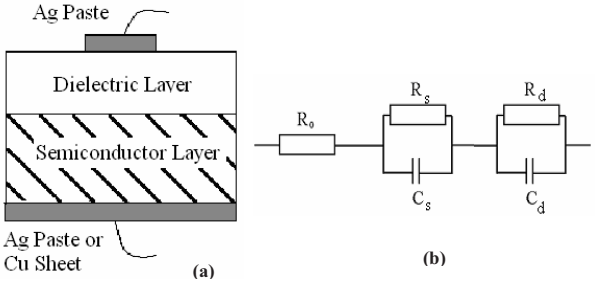


Figure 1 (a) Schematic diagram of the organic capacitor; (b) circuit model for describing the dielectric behavior of organic capacitor, where $R_0$ is the sum of interface resistance, $R_s$ and $C_s$ are the resistance and capacitance of semiconductor layer, and $R_d$ and $C_d$ are the resistance and capacitance of dielectric layer, respectively.

## 3 RESULTS AND DISCUSSION

Relaxation of the impedance can be ideally illustrated with Debye's expression, where the material is represented by a parallel circuit with a pure resistor R and a capacitor C. Therefore, the impedance behavior of organic capacitor can be described by a series of double parallel RC circuit elements [13] that correspond to the dielectric behavior of the semiconductor and dielectric layers, respectively, as shown in Figure 1(b). Here the resistor R represents ionic or electronic conduction mechanisms, while the capacitor C represents the polarizability of the organic materials. The complex impedance Z* measured can be expressed as

$$\begin{cases} Z^* = Z' - jZ'' \\ Z' = R_0 + \dfrac{R_s}{1+\omega^2 R_s^2 C_s^2} + \dfrac{R_d}{1+\omega^2 R_d^2 C_d^2} \\ Z'' = \dfrac{\omega R_s^2 C_s}{1+\omega^2 R_s^2 C_s^2} + \dfrac{\omega R_d^2 C_d}{1+\omega^2 R_d^2 C_d^2} \end{cases} \quad (1)$$

where $Z'$ and $Z''$ represent the real and imaginary parts of the impedance and $\omega$ is the angular frequency. For the semiconductor layer, its resistivity is low while that of the dielectric layer is much higher. It is thus thought that, in high frequency region, $\omega^2 R_d^2 C_d^2 >> 1$, while $\omega^2 R_s^2 C_s^2 \sim 1$, the equation (1) can hence be expressed as

$$\begin{cases} Z' = R_0 + \dfrac{R_s}{1+\omega^2 R_s^2 C_s^2} + \dfrac{1}{\omega^2}\dfrac{1}{R_d C_d^2} \\ Z'' = \dfrac{\omega R_s^2 C_s}{1+\omega^2 R_s^2 C_s^2} + \dfrac{1}{\omega}\dfrac{1}{C_d} \approx \dfrac{1}{\omega}\dfrac{1}{C_d} \end{cases} \quad (2)$$

When frequency is further decreased but $\omega^2 R_d^2 C_d^2 >> 1$ and $\omega^2 R_s^2 C_s^2 << 1$, the equation (1) is given as

$$\begin{cases} Z' = R_0 + R_s + \dfrac{1}{\omega^2}\dfrac{1}{R_d C_d^2} \\ Z'' = \omega R_s^2 C_s + \dfrac{1}{\omega}\dfrac{1}{C_d} \approx \dfrac{1}{\omega}\dfrac{1}{C_d} \end{cases} \quad (3)$$

The equation (2) and (3) can well explain the response of real and imaginary parts of impedance of an organic capacitor in high frequency ($10^5$–$10^6$ Hz), as shown in Figure 2. In lower part of high frequency region, the Z' is linearized with $1/\omega^2$. When frequency is increased, the impedance behavior of semiconductor layer is largely affected by frequency and thus Z' increases non-linearly with $1/\omega^2$.

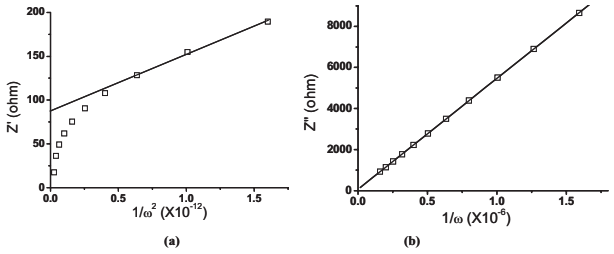


Figure 2 Response of real and imaginary parts of impedance in high frequency (105–106 Hz).

The way [14] by which to extract the capacitance and resistance of the dielectric layer uses the equation (3) in high–frequency range ($10^5$–$10^6$ Hz). The capacitance $C_d$ is given by the slope of the straight line determined by the variation of Z" as a function of $1/\omega$. Resistance $R_d$ is calculated from $C_d$ and the slope of straight line determined by the variation of Z' as a function of $1/\omega^2$ in the linear region. Then, the dielectric constant $\varepsilon_d$ and conductivity $\sigma_d$ of the dielectric layer are calculated based on the equation: $\varepsilon_d = C_d l/(\varepsilon_0 S)$ and $\sigma_d = l/(R_d S)$. $\varepsilon_0$ is the dielectric constant of a vacuum, l is the thickness of the sample that was measured upon cross section of the sample by SEM; S is the area of silver electrode.

It has often argued that a positive $d\sigma/dT$ necessarily implies that the system is non-metallic or at any rate close to a transition while the system with negative $d\sigma/dT$ tends to metallic[15-17]. Figure 3 (a) shows the conductivity variation for two kinds of dielectric materials with the

temperature increase. The behavior of Urathan can be thought as non-
metallic and the enhancement in conductivity by heating with an activation energy transition originates from hopping mechanism that occurs around the Fermi edge, as introduced in following part. Material 2, DuPont 5018A tends to be metallic at high temperature and the $d\sigma/dT$ changes from positive to negative is due to carrier diffusion effects [16]. Furthermore, the interface resistance $R_0$ can be derived from equation (2) and (3). The interface resistance between Urathan and semiconductor layer is ~20 ohm which is lower than the value for material 2 (~600 ohm). When these two materials are assessed as dielectric layer in OFET, Urathan, due to its lower conductivity, non-metallic conduction behavior at high temperature and lower interface resistance, is more suitable as the dielectric layer than material 2.

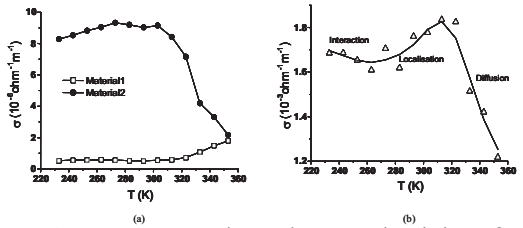


Figure 3 Temperature-dependent conductivity of dielectric (a) semiconductor (b) materials

Figure 3(b) shows the conductivity variation for an organic semiconductor material at different temperatures. The curves obtained here is very similar to the reported temperature-dependent conduction behavior of metallic disordered systems [16] in which σ changes its slope three time and the different σ variation behaviors are attributed to electron interaction effect, localization effect and diffusion effect, respectively. In organic conductive polymers, carrier densities in the range of $10^{12}$–$10^{14}$cm$^{-3}$ have been observed [18]. Therefore, we estimate that the carrier mobility of this kind of semiconductor material is ~1 $cm^2V^{-1}s^{-1}$ supposing the carrier density is $10^{14}cm^{-3}$. This value is similar to reported mobility of organic materials such as N-isopropylcarbazole [19], anthracene [20] and naphthalene [21], and Durene, etc.

It is known that the electrical conductivity of non-metallic materials is usually thermally activated, at least over a limited temperature and follows Arrhenius law,

$$\sigma_d = \sigma_c \exp(-\frac{E_a}{k_B T}) = \sigma_c \exp(-\frac{E_{TR} - E_F}{k_B T}) \qquad (4)$$

where $\sigma_c$ is a pre-exponential factor and is characteristics of the material. $E_{TR}$ is defined as the average energy of the conducting electrons. Ea, EF, $k_B$, and T are, respectively, the activation energy for conduction, Fermi energy, Boltzmann's constant, and absolute temperature. Thus, the activation energy for conduction can be calculated from the slope of the straight line given by least-mean-square analysis of $\ln\sigma_d$ vs 1000/T as shown in Figure 4(a). The activation energy for conduction of Urathan is found to have a transition from 0.002 to 0.24 eV at about $307^0$K. Several researchers have proposed different mechanisms for the conduction transition of materials with a rise in temperature. Landstrass and Ravi [22] attributed the transition to the movement of hydrogen and defects from the electrically active deep level to nonactive sites during annealing. Mori et al. [23] suggested an existence of a surface conductive layer combined with chemical absorption and oxidation. Bharadwaja and Krupanidhi [24] proposed that the transition originated from the excitation of charge carriers from a set of shallow traps lying below the conduction band and/or oxygen ion mobility in the interior grains. Axelrod et al [6] correlated the transition to the fractal geometry of materials and to thermally activated relaxation processes from localized and delocalized electronic states of nanocrystallites below the Fermi edge. Here we propose this conduction transition behavior of organic material originates from band tail hopping that occurs around the Fermi edge, as illustrated in Figure 4(b).

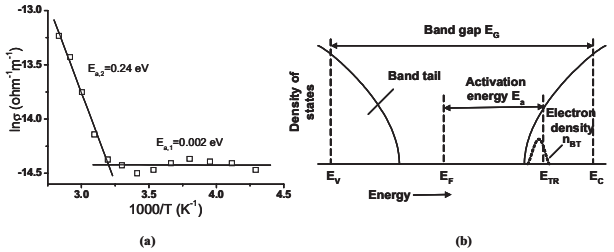


Figure 4 (a) Arrhenius plot of the conductivity of Urathan with an activation energy transition from 0.002 to 0.24 eV at about 307 K. (b) Schematic diagram of the distribution of the density of states showing the conductivity activation energy Ea, the average conduction energy ETR, and the Fermi energy EF (after Ref.[25] ).

It is known that the Fermi edge lies between the valence band (i.e. highest occupied molecular orbital (HOMO)) and conduction band (i.e. lowest unoccupied molecular orbital (LUMO)). Because the band gap of organic dielectric materials is very large, it is very difficult for electrons to overcome the energy gap and transport from valence band to conduction band. Hence the main mechanism responsible for the conductivity of dielectric layer is the band tail hopping, i.e. the electrons are transported from the Fermi edge to the conduction band tail. The inflexion $307^0$K can be viewed as the equilibration temperature at which a high temperature equilibrium regime and a low temperature frozen state are separate. The different variation in conductivity for the temperature above and below this critical point is due to changes in the electron concentration. Below the equilibration temperature, the electronic structure of dielectric layer is frozen and the density of electrons is constant. Hence $E_{TR}$ is close to $E_F$ and the corresponding activation energy is very small.

Furthermore, the conductivity prefactor $\sigma_c$ is only about $5.7\times10^{-7}$ $\Omega^{-1}$ $m^{-1}$ as derived from the vertical intercept in Figure 4(a). When the temperature is raised above the equilibration temperature, the electrons near the Fermi edge are excited towards higher energy and $E_{TR}$ shifts into the band tail near $E_C$ while the Fermi energy is pinned by the defect and dopant states due to the thermal equilibrium regime at every temperature and consequently the shift of the Fermi edge is comparatively small. As a result, the conductivity is activated with much larger activation energy and a prefactor of about 0.006 $\Omega^{-1}$ $m^{-1}$.

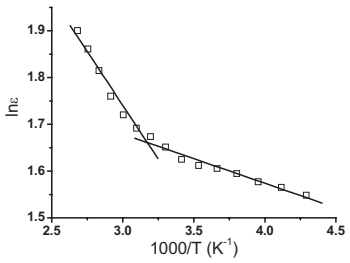


Figure 5 Plot of $\varepsilon_d$ of Urathan vs 1000/T with a transition at about 314 K.

The correlation between $\varepsilon_d$ of Urathan and the temperature is plotted in Figure 5. It can be observed that there is also a transition at about 314 K which is very similar to the curve of the conduction transition. $\varepsilon_d$ is subsequently expressed in exponential form as $\varepsilon_d = \varepsilon_c \exp(-\beta/T)$. The coefficient β increases from 111 to 445 $K^{-1}$ and $\varepsilon_c$ from 6.9 to 20.2 at the equilibration temperature. The transition typically suggests the presence of specific polarization phenomenon: electronic polarization associated to band tail hopping, which contributes to the rapid rise of dielectric constant above the equilibration temperature. Electron–phonon interaction allows the charge to locally distort the structure around it and subsequently trap itself in the resulting potential well, which results in the polaron formation [26].

Using the two dielectric materials and the semiconducting active material, two OFETs were fabricated. The results obtained from the OFETs were well in agreement with the conclusion drawn from the fabricated organic transistors and corresponding analysis.

## 4 CONCLUSION

A new impedance analysis method has been developed to distinguish the individual contributions to electrical conduction and dielectrics and derives useful information on conductivity, conduction behavior at high temperature and interface resistance, which can become a simple standard in assessing the materials for OFETs. Urathan which is more suitable as dielectric layer based on this standard appears an enhancement in conductivity by heating following an Arrhenius law with an activation energy transition from 0.002 to 0.24 eV at ~$307^0$K, which originates from band tail hopping that occurs around the Fermi edge. At ~$314^0$K, a dielectric transition also occurs. This transition behavior is interpreted as a combination of electron polarization associated to the band tail hopping.

## REFERENCES


[1] Butko, V. Y.; Chi, X.; Lang, D. V.; Ramirez, A. P. Appl. Phys. Lett. 83, 4773, 2003.

[2] Schauer, F. J. Appl. Phys. 86, 524,1999.

[3] Schon, J. H.; Berg, S.; Kloc, Ch.; Batlogg, B. Science 287, 1022, 2000.

[4] Lanfredi, S.; Rodrigues, A. C. M. J. Appl. Phys. 86, 2215,1999; Ivanov, D.; Caron, M.; Ouellet, L.; Blain, S.; Hendricks, N.; Currie, J. ibid. 77, 2666, 1995.

[5] H. Kakiuchida, K. Saito, and A. J. Ikushima, J. Appl. Phys. 11, 5983, 1999.

[6] Axelrod, E.; Givant, A.; Shappir, J.; Feldman, Y.; Sa'ar, A. Phys. Rev. B 65, 165429, 2002; J. Non-Cryst. Solids, 305, 235, 2002.

[7] Ye, H. T.; Sun, C. Q.; Huang, H. T.; Hing, P. Appl. Phys. Lett. 78, 1826, 2001.

[8] Pan, L. K.; Huang, H. T.; Sun, C. Q. J. Appl. Phys. 94, 2695, 2003.

[9] Inzelt, G.; Lang, G.; Kertesz, V.; Bacskai, J. Electrochim. Acta 38, 2503, 1993.

[10] Bassiouni, M. E.; Al-Shamy, F.; Madi, N. K.; Kassem, M. E. Mater. Lett. 2003, 57, 1595.

[11] Florit, M. I. J. Electroanal. Chem. 408, 257, 1996.

[12] Hirose, N.; West, A. R. J. Am. Ceram. Soc. 76, 1633, 1996.

[13]Macdonald, J. R. Impedance Spectroscopy; Wiley: New York, 1987; Chap. 4.

[14]Lanfredi, S.; Carvalho, J. F.; Hernandes, A. C. J. Appl. Phys. 88, 283, 2000.

[15]Enderby, J. E.; Barnes, A. C. J. Phys. Conds. Matter 12, A181, 2000.

[16]Kaveh, M.; Mott, N. F. J. Phys. C: Solid State Phys. 15, L707, 1982.

[17]Bohm, M. C.; Staib, A. Phys. Rev. B 18, 11930, 1990.

[18]Szymanski, A. Bull. Acad. Polon. Sci. Ser. Sci. Math. Astron. Phys. 16, 149, 1968.

[19] Sharp, J. H. Phot. Sci. Eng. 11, 69, 1967.

[20] Katz, J. L.; Rice, S. A.; Choi, S. I.; Jortner, J. J. Chem. Phys. 39, 1683, 1963.

[21] Burshtein, Z.; Williams, D. F. J. Chem. Phys. 66, 2746, 1977.

[22] Lanstrass, M. I.; Ravi, K. V. Appl. Phys. Lett. 55, 1391, 1989.

[23] Mori, Y.; Eimori, N.; Hatta, A.; Ito, T.; Hiraki, A. Jpn. J. Appl. Phys. Part 2, 31, L1718, 1992.

[24]Bharadwaja, S. S. N. ; Krupanidhi, S. B. Mater. Sci. En., B 78, 75, 2000.

[25]Street, R. A "Hydrogenated Amorphous Silicon" Cambridge University Press: Cambridge, 227, 1991.

[26]Jung, W. H. J. Appl. Phys. 90, 2455, 2001.